CERN-TH/2002-148
FTUAM-02-18
IFT-UAM/CSIC-02-26
FTUV-02-0704
IFIC/02-27

Superbeams plus Neutrino Factory: the golden path to leptonic CP violation

J. Burguet-Castell[a,], M.B. Gavela[b,1], J.J. Gómez-Cadenas[a,c2], P. Hernández[c,3], O. Mena[b,4]

[a] Dept. de Física Atómica y Nuclear and IFIC, Universidad de Valencia, Spain
[b] Dept. de Física Teórica, Univ. Autónoma de Madrid, Spain
[c] CERN, 1211 Geneva 23, Switzerland

Abstract

Superbeams (SB) and Neutrino Factories (NF) are not alternative facilities for exploring neutrino oscillation physics, but successive steps. The correct strategy is to contemplate the combination of their expected physics results. We show its important potential on the disappearance of fake degenerate solutions in the simultaneous measurement of θ_{13} and leptonic CP violation. Intrinsic, sign(Δm^2_{13}) and θ_{23} degeneracies are shown to be extensively eliminated when the results from one NF baseline and a SB facility are combined. A key point is the different average neutrino energy and baseline of the facilities. For values of θ_{13} near its present limit, the short NF baseline, e.g. $L = 732$ km, becomes, after such a combination, a very interesting distance. For smaller θ_{13}, an intermediate NF baseline of O(3000km) is still required.

1 Introduction

Recent data [1] strongly favour the large mixing angle solution (LMA-MSW) [2] to the solar neutrino deficit [3]. This, if confirmed, is very good news as regards the prospects of discovering leptonic CP violation. The measurement of the angle θ_{13} and the CP-odd phase δ would be possible at a superbeam (SB) facility [4, 5, 6] or/and a neutrino factory (NF) [7], mainly through $\nu_\mu \leftrightarrow \nu_e$ and $\bar{\nu}_\mu \leftrightarrow \bar{\nu}_e$ oscillations, provided θ_{13} is not too small. How "small" is one of the points to be quantified below.

[1] gavela@delta.ft.uam.es
[2] gomez@hal.ific.uv.es
[3] pilar.hernandez@cern.ch. On leave from Dept. de Física Teórica, Universidad de Valencia.
[4] mena@delta.ft.uam.es

The development of a neutrino factory requires, by design, the essentials of a superbeam facility as an intermediate step. Although the ultimate precision and discovery goals in neutrino oscillation physics may only be attained with a neutrino factory from muon storage rings, those "for free" superbeam results can already lead to significant progress in central physics issues such as those mentioned above.

Superbeams and neutrino factory are thus not alternative options, but successive steps. In this perspective, the correct analysis strategy is to contemplate the combination of their expected physics results. We will take such a step here and show its important impact, in particular on the disappearance of fake solutions in the simultaneous measurement of θ_{13} and δ.

It was shown in ref. [8] that there exists generically, at a given (anti)neutrino energy and fixed baseline, a second value of the set $(\theta_{13}^{'}, \delta^{'})$ that gives the same oscillation probabilities for neutrinos and antineutrinos as the true value chosen by nature. In what follows, these fake solutions will be dubbed *intrinsic degeneracies*.

More recently it has been pointed out [9] that other fake solutions might appear from unresolved degeneracies in two other oscillation parameters:

- the sign of Δm^2_{13},
- θ_{23}, upon the exchange $\theta_{23} \leftrightarrow \pi/2 - \theta_{23}$ for $\theta_{23} \neq \pi/4$.

It is not expected that these degeneracies will be resolved before the time of the SB/NF operation. However, the subleading transitions $\nu_e \leftrightarrow \nu_\mu$, from which the parameters θ_{13} and δ can be measured, are sensitive to these discrete ambiguities. A complete analysis of the sensitivity to the set (θ_{13}, δ) should therefore assume that sign(Δm^2_{13}) can be either positive or negative and $\theta_{23} >$ or $< \pi/4$. If a wrong choice of these possibilities cannot fit the data, the ambiguities will be resolved, else they will generically give rise to new fake solutions for the parameters θ_{13} and δ.

Strategies to eliminate some of the fake solutions have previously been discussed, advocating the combination of different baselines [8], an improved experimental technique allowing the measurement of the neutrino energy with good precision[10], the supplementary detection of $\nu_e \to \nu_\tau$ channels [11] and a cluster of detectors at a superbeam facility located at different off-axis angles, so as to have different $\langle E \rangle$ [12].

We consider the three types of degeneracies as they would appear in the analysis from the data taken at a neutrino factory and at an associated superbeam. We then show the potential of combining their results. For the NF we consider the experimental setup presented in [13, 14, 8]. The parent $\mu^\pm$ energy is 50 GeV and the reference baselines considered will be 732 and 2810 km. As the SB facility we consider the design proposed for the CERN SPL [15], which could be the initial step of a NF based at CERN. The average energy is $\langle E_\nu \rangle = 0.25$ GeV and the baseline is $L = 130$ km (CERN-Fréjus). The fluxes and detector systematics have been discussed in [6]. In the detailed computations of this paper we will not consider other types of superbeams, such as JHF [16], nor the case of beta-beams [17], although we will also discuss the potential of these alternative experimental setups in this context.

Whenever it is not specified otherwise, we take the following central values for the oscillation parameters: $\sin 2\theta_{12}$.$\Delta m^2_{12} = 10^{-4}$eV^2 with $\Delta m^2_{12} > 0$, $|\Delta m^2_{13}| = 3 \times 10^{-3}$ eV^2 and

$\sin 2\theta_{23} = 1$. Some implications of making them vary within their currently allowed ranges will be discussed as well. The errors expected in the knowledge of these parameters, as well as the error in the matter profile of the Earth will not be included. We previously studied their impact in ref. [8] and they are not expected to change the conclusions significantly.

2 Degenerate solutions

In this study we will consider in detail the measurement of the subleading probabilities $P_{\nu_e\nu_\mu(\bar\nu_e\bar\nu_\mu)}$ in the NF complex, through the detection of "wrong-sign" muons, and $P_{\nu_\mu\nu_e(\bar\nu_\mu\bar\nu_e)}$ in the SB facility, through the detection of electrons/positrons.

For the energies and baselines under discussion, the oscillation probabilities in vacuum are accurately given by (for more details see [14]):

$$\begin{aligned} P_{\nu_e\nu_\mu(\bar\nu_e\bar\nu_\mu)} &= s_{23}^2 \sin^2 2\theta_{13} \sin^2\left(\frac{\Delta m_{13}^2 L}{4E}\right) + c_{23}^2 \sin^2 2\theta_{12} \left(\frac{\Delta m_{12}^2 L}{4E}\right)^2 \\ &+ \tilde J \cos\left(\delta \mp \frac{\Delta m_{13}^2 L}{4E}\right) \frac{\Delta m_{12}^2 L}{4E} \sin \frac{\Delta m_{13}^2 L}{4E} \ , \end{aligned} \tag{1}$$

where $\tilde J$ is defined as

$$\tilde J \equiv \cos\theta_{13} \ \sin 2\theta_{13} \ \sin 2\theta_{23} \ \sin 2\theta_{12}. \tag{2}$$

The vacuum approximation should be excellent as regards the SB scenario with a baseline of hundreds of kilometers, while in practice it also gives a good indication for the results at the short (732 km) and intermediate (2000–3000km) baselines of a NF. Of course all the fits below include the exact formulae for the probabilities, including matter effects.

As in ref. [8], we will denote the three terms in eq. (1), atmospheric, solar and interference, by $P^{atm}_{\nu(\bar\nu)}$, P^{sol} and $P^{inter}_{\nu(\bar\nu)}$, respectively. When θ_{13} is relatively large or $|\Delta m_{12}^2|$ small, the probability is dominated by the atmospheric term. We will refer to this situation as the atmospheric regime. Conversely, when θ_{13} is very small or $|\Delta m_{12}^2|$ large (with respect to $\langle E_\nu\rangle/L$ and $|\Delta m_{13}^2|$), the solar term dominates $P^{sol} \gg P^{atm}_{\nu(\bar\nu)}$. This is the solar regime. The interference term, which contains the information on the CP-violating phase δ, can never dominate since

$$|P^{inter}_{\nu(\bar\nu)}| \le P^{atm}_{\nu(\bar\nu)} + P^{sol}. \tag{3}$$

It is precisely in the transition between the two regimes where the interference term becomes larger in relative terms. There the corresponding CP-odd asymmetry becomes maximal and independent of the precise value of the two small parameters: Δm_{12}^2 and θ_{13} [8]. As an indication, for the solar parameters $\sin 2\theta_{12} \cdot \Delta m_{12}^2 = 10^{-4}$ eV^2, the transition is at $\theta_{13} \simeq 1^\circ$ for the NF setups considered here and $\theta_{13} \simeq 2^\circ$ for the SPL-SB facility.

3 Intrinsic degeneracies

In a previous work [8] we uncovered, at fixed neutrino energy and baseline, the existence of degenerate solutions in the (θ_{13}, δ) plane for fixed values of the oscillation probabilities $\nu_e(\bar\nu_e) \to \nu_\mu(\bar\nu_\mu)$. If (θ_{13}, δ) are the values chosen by nature, the conditions

$$\left.\begin{array}{l} P_{\nu_e\nu_\mu}(\theta_{13}^{'}, \delta^{'}) = P_{\nu_e\nu_\mu}(\theta_{13}, \delta) \\ P_{\bar\nu_e\bar\nu_\mu}(\theta_{13}^{'}, \delta^{'}) = P_{\bar\nu_e\bar\nu_\mu}(\theta_{13}, \delta) \end{array}\right\} \quad (4)$$

can be generically satisfied by another set $(\theta_{13}^{'}, \delta^{'})$. Using the approximate formulae of eq. (1), it is easy to find the expression for these *intrinsic* degeneracies deep in the atmospheric and solar regimes. In ref. [8] the general results including matter effects were presented. Here we just recall the solutions in vacuum, which are simpler and accurately describe the new situation considered here, that of the superbeams.

For θ_{13} sufficiently large and in the vacuum approximation, apart from the true solution, $\delta^{'} = \delta$ and $\theta_{13}^{'} = \theta_{13}$, there is a fake one at

$$\begin{aligned} \delta^{'} &\simeq \pi - \delta, \\ \theta_{13}^{'} &\simeq \theta_{13} + \cos\delta\ \sin 2\theta_{12}\, \frac{\Delta m_{12}^2 L}{4E} \cot\theta_{23} \cot\left(\frac{\Delta m_{13}^2 L}{4E}\right) \quad . \end{aligned} \quad (5)$$

Note that for the values $\delta = -90°, 90°$, the two solutions degenerate into one. Typically $\cot\left(\frac{\Delta m_{13}^2 L}{4E}\right)$ has on average opposite signs for the proposed SB and the NF setups[5], for $\Delta m_{13}^2 = 0.003$ eV^2:

	$\langle E\rangle$(GeV)	L(km)	$\cot\left(\frac{\Delta m_{13}^2 L}{4E}\right)$
SB − SPL	0.25	130	−0.43
JHF − off − axis	0.7	295	−0.03
NF@732	30	732	+10.7
NF@2810	30	2810	+2.68
$\beta-$beam	0.35	130	+0.17

When $\theta_{13} \to 0$ and in the vacuum approximation, the intrinsic degeneracy is independent[6] of δ:

$$\left.\begin{array}{l} \text{if } \cot\left(\frac{\Delta m_{13}^2 L}{4E}\right) > 0 \text{ then } \delta^{'} \simeq \pi \\ \text{if } \cot\left(\frac{\Delta m_{13}^2 L}{4E}\right) < 0 \text{ then } \delta^{'} \simeq 0 \end{array}\right\} \quad \theta_{13}^{'} \simeq \sin 2\theta_{12}\ \frac{\Delta m_{12}^2 L}{4E}\ |\cot\theta_{23}\ \cot\left(\frac{\Delta m_{13}^2 L}{4E}\right)\ |. \quad (6)$$

This solution was named $\theta_{13} = 0$-mimicking solution and occurs because there is a value of $\theta_{13}^{'}$ for which there is an exact cancellation of the atmospheric and interference terms in both the neutrino and antineutrino probabilities simultaneously, with $\sin\delta' = 0$.

Figure 1 shows the results of measuring (θ_{13}, δ) at the SPL-SB facility, for $\theta_{13} = 8°$ and the central values of $\delta = -180, -90, 90, 180°$. The intrinsic degeneracies clearly appear and are well described by eqs. (5). The details of the analysis can be found in ref. [6]. We simply

[5]Clearly the parameters for these setups are not fixed yet and might be modified conveniently in the final designs.

[6]All throughout this paper we will only consider those fake solutions which lie inside the experimentally allowed range for θ_{13}.

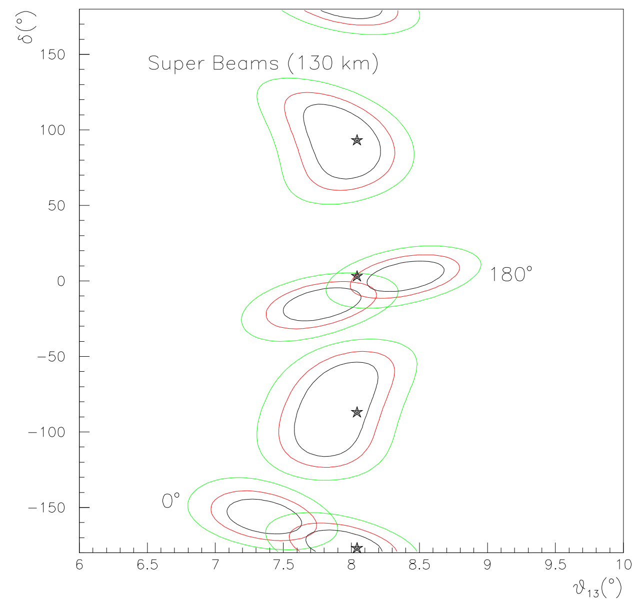

Figure 1: *Fits to given true (nature) solutions and their intrinsic degenerate solutions at a SB facility. The* 68.5%, 90% *and* 99% *contours are depicted, for four central values of* $\delta = -90°, 0°, 90°, 180°$ *and for* $\theta_{13} = 8°$.

stress here that the analysis is based on the total number of electron/positron events, so we do not assume that the neutrino energy can be reconstructed. Our results about the NF can be found in ref. [8], where it was shown that these intrinsic degeneracies also could not be resolved in a single baseline, in spite of the spectral information, although they did get eliminated when two NF baselines (intermediate and long) were combined [7]. A comparison of the NF and SPL-SB fits shows that the displacement of the fake solution with respect to the true one is opposite for the two facilities.

In order to understand the intermediate region between the solar and atmospheric regimes, as well as the influence of matter effects, we have determined numerically all the possible physical solutions to eqs. (4), using the approximate formulae for the probabilities including matter effects [14]. L and E are fixed to the average values for the different facilities. The results for the shift $\theta_{13}' - \theta_{13}$ and δ' are shown in Fig. 2 as a function of θ_{13}, for two values of $\delta = 0°, 90°$ and for the different experimental setups. In the whole range of parameters we find two solutions, as expected by periodicity in δ, since one solution is warranted: the true one.

The most important point to note in eqs. (5) and (6) and in Figs. 2 is that the position (measured in $\theta_{13}' - \theta_{13}$ or δ') of the degenerate solution is very different in the NF, the SPL-

[7]The authors of [10] did not find intrinsic degeneracies in their simulations by assuming a very optimistic lower cut in the momentum of the muon.

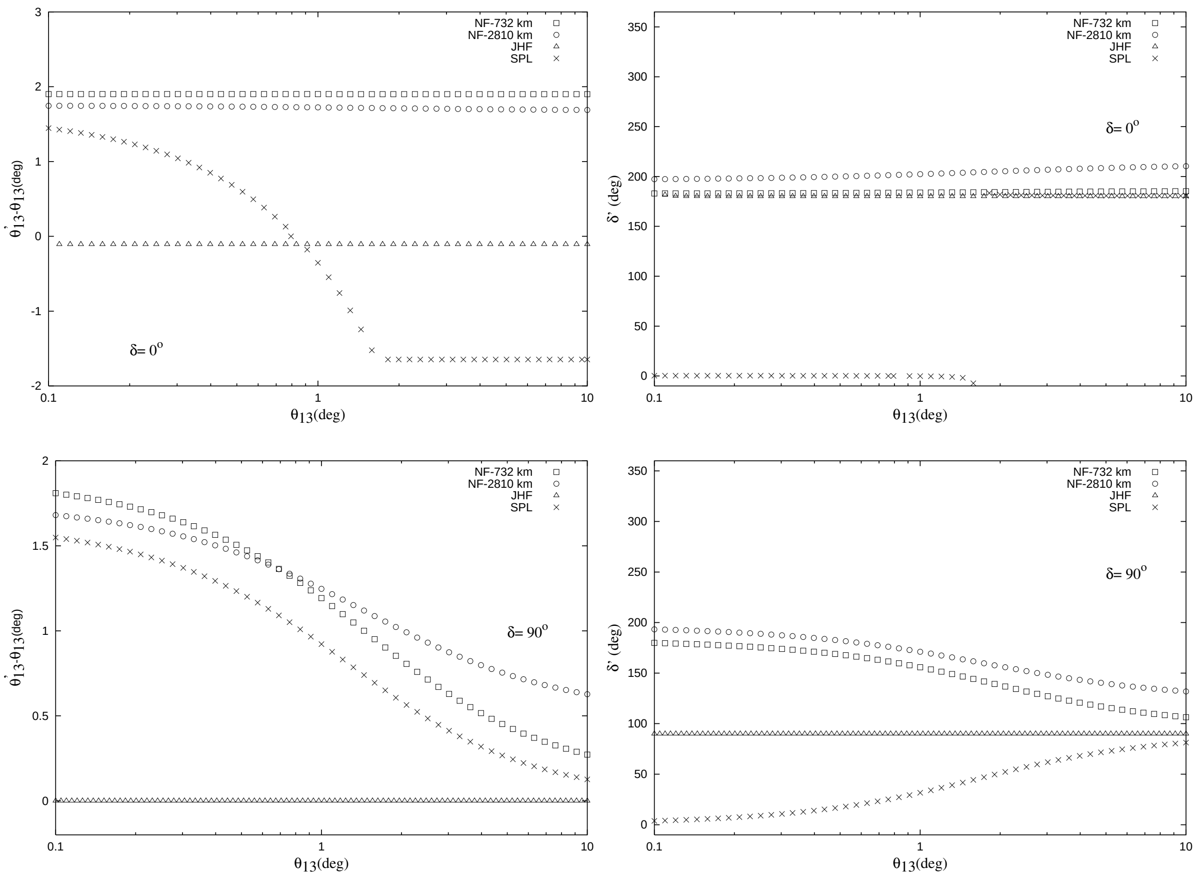

Figure 2: $\theta_{13}^{'} - \theta_{13}$ *(left) and* δ' *(right) versus* θ_{13}*, for the intrinsic fake solution, for fixed values of* $\delta = 0^\circ$ *(up) and* $\delta = 90^\circ$ *(down).*

SB and JHF[8] setups. As a result, we expect that any combination of the results of two of these three facilities could in principle exclude the fake solutions. The $\theta_{13}^{'} - \theta_{13}$ of the fake solution depends strongly on the baseline and the neutrino energy through the ratio L/E, so the combination of the results of two experiments with a different value for this ratio should be able to resolve these degeneracies, within their range of sensitivity. Even more important is that, for small θ_{13}, δ' may differ by 180° if the two facilities have opposite sign for $\cot\left(\frac{\Delta m_{13}^2 L}{4E}\right)$, see eqs. (6). For the NF setups, this sign is clearly positive, since the measurement of CP violation requires, because of the large matter effects, a baseline considerably shorter than that corresponding to the maximum of the atmospheric oscillation (in vacuum), where the cotangent changes sign. In the SB scenario on the other hand, because of the smaller $\langle E \rangle$, matter effects are small at the maximum of the atmospheric oscillation, which then becomes the optimal baseline for CP violation studies. It is then not very difficult

[8] For the JHF scenario the shift in θ_{13} is minimal because for the reference parameters $\langle E_\nu \rangle = 0.7$ GeV and $L = 295$ km, $\cot\left(\frac{\Delta m_{13}^2 L}{4E}\right) \simeq 0$.

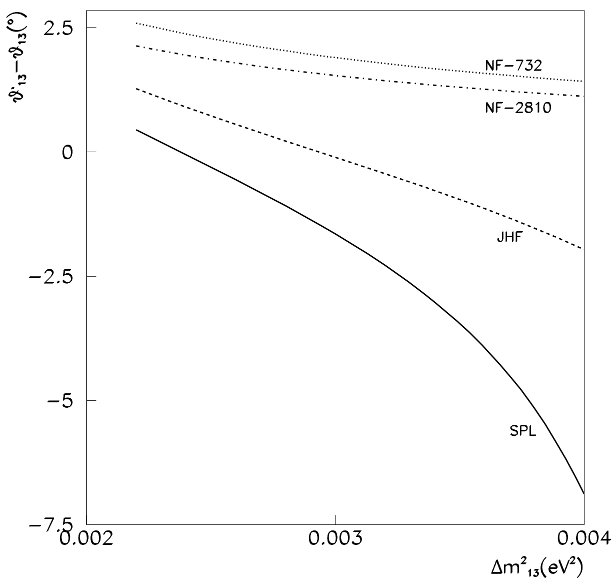

Figure 3: $\theta'_{13} - \theta_{13}$ *versus* $|\Delta m^2_{13}|$ *for the intrinsic fake solution in the atmospheric regime and* $\delta = 0°$.

to ensure that cot $\left(\frac{\Delta m^2_{13} L}{4E}\right)$ be dominantly negative in this case[9], which results in an optimal complementarity of the two facilities in resolving degeneracies.

Clearly the position of the fake solution is very sensitive to the atmospheric $|\Delta m^2_{13}|$. In matter we expect a milder dependence, especially if matter effects become dominant. In Fig. 3 we show the separation in θ_{13} of the intrinsic degenerate solution at $\delta = 0°$ in the atmospheric regime as a function of $|\Delta m^2_{13}|$. Although in general the separation becomes smaller for smaller $|\Delta m^2_{13}|$, it is sizeable in the whole allowed range. The relative difference between the results for the NF facility and the SPL superbeam option is always largest, although the differences between the two superbeams and that between the NF and JHF are also very large. Note also that the sign of ${\theta_{13}}' - \theta_{13}$, which is related to that of cot $\left(\frac{\Delta m^2_{13} L}{4E}\right)$, is positive in all the domain for the NF baselines and negative in most of the domain for SPL-SB scenario, which implies that the difference in δ' between the two facilities is 180° for small θ_{13}. For JHF, it is negative only for $|\Delta m^2_{13}| \geq 0.003$ eV^2.

Concerning the dependence on the solar parameters, it enters only through the combination $\sin 2\theta_{12} \, . \frac{\Delta m^2_{12} L}{4E}$. In general $\theta'_{13} - \theta_{13}$ is linear in this quantity, so degenerate solutions become closer with smaller Δm^2_{12} and also closer to the true solution. Note however that δ' in the solar regime does not depend on the solar parameters and that it differs by 180° in the two facilities, and this separation will remain when Δm^2_{12} is lowered.

[9]Note however that the neutrino beams are generally broad so it is necessary for this argument to hold that most of the events have a parent neutrino energy giving the appropiate sign. The results of the fits indicate that this is the case in the two facilities (NF and SPL-SB) that are considered in detail.

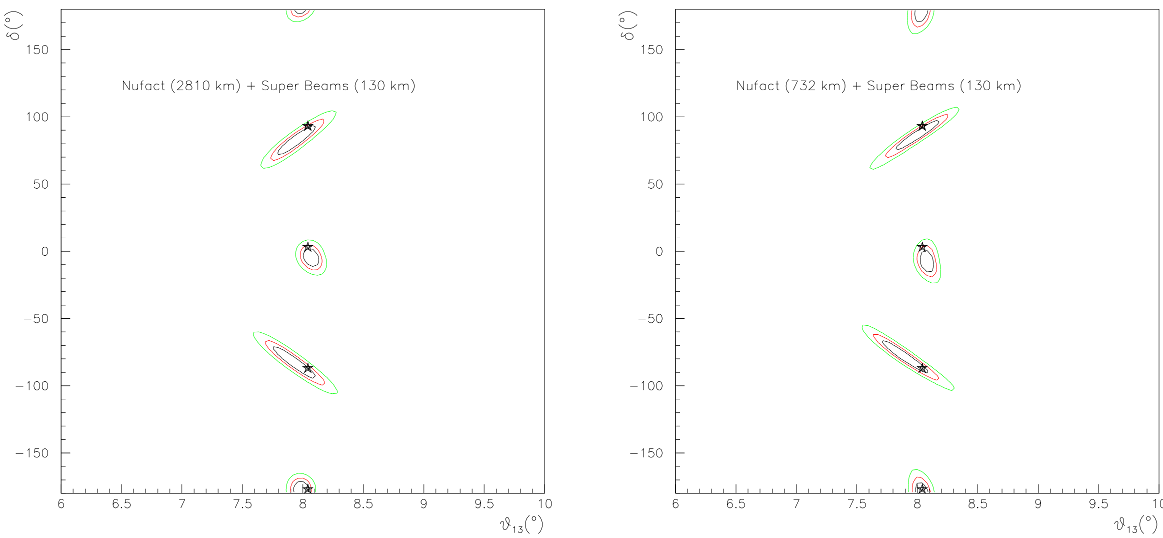

$\theta_{13} = 8°$

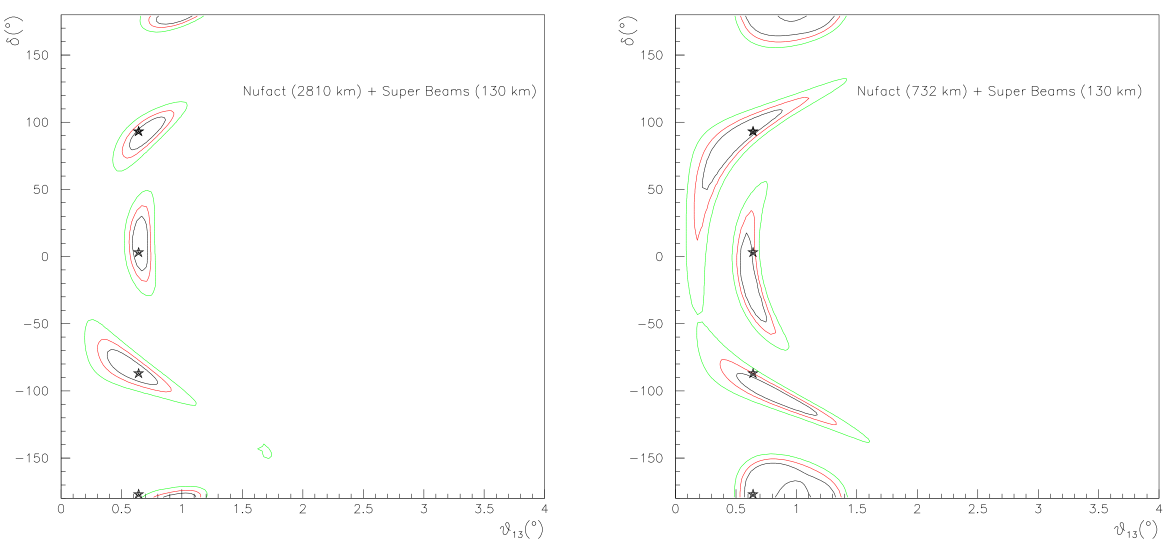

$\theta_{13} = 0.6°$

Figure 4: *Fits combining the results from the SPL-SB facility and a NF baseline at $L = 2810$ km (left) or $L = 732$ km (right). The true values illustrated correspond to $\delta = -90°, 0°, 90°, 180°$ and $\theta_{13} = 8°$ (top) or $\theta_{13} = 0.6°$ (bottom). Notice that the fake intrinsic solutions have completely disappeared in the combinations.*

Turning to the variation of the solar parameters while in the atmospheric regime, we will now argue that, if the two facilities that are combined have opposite sign$(\cot \frac{\Delta m^2_{13} L}{4E})$, the effect of lowering Δm^2_{12} is not dramatic either in the resolution of degeneracies. The statistical error on the measurement of θ_{13} and δ is mainly independent of the solar parameters (it is dominated by the atmospheric term), which means that at some point when Δm^2_{12} is lowered, the degenerate solutions of the two facilities will merge, since the error remains constant while the separation of the solutions gets smaller. However, because of the opposite sign of ${\theta_{13}}' - \theta_{13}$, the solutions of the two facilities will merge only when they merge with the true solution in θ_{13}. If this happens, it would therefore not bias the measurement of θ_{13} and δ.

We have performed a detailed combined analysis of the NF results [14, 8] and those from the SPL-SB [6] facility. The combination with the optimal NF baseline $L = 2810$ km is sufficient to get rid of all the fake solutions, as shown in Figs. 4 (left). Note that indeed the disappearance of the fake solutions takes place even in the solar regime!

One very interesting exercise is to reconsider the combination of the SPL-SB and the NF results at a shorter baseline of $L = 732$ km. As explained in refs. [14, 8], the degenerate solution is not so relevant to this NF baseline when considered alone, because there the sensitivity to CP violation is so poor that there exists a continuum of almost degenerate solutions, which makes the determination of δ impossible with the wrong-sign muon signals. The combination of the results from this NF baseline with those from the SPL-SB facility is summarized in the tantalizing plots in Figs. 4 (right). Not only do the fake solutions corresponding to the intrinsic degeneracies in the superbeam disappear, but the accuracy in the determination of the true solution becomes competitive with that obtained in the combination with the optimal baseline for large values of θ_{13}. At small values of θ_{13} the latter still gives better results, as expected.

4 sign(Δm^2_{13}) degeneracy

Assume nature has chosen a given sign for Δm^2_{13}, while the data analysis is performed assuming the opposite sign. Let us call $P^{'}_{\nu_e\nu_\mu(\bar\nu_e\bar\nu_\mu)}(\theta_{13}, \delta)$ the oscillation probability with the sign of Δm^2_{13} reversed. We may then get new fake solutions $({\theta_{13}}', \delta')$, at fixed E_ν and L, if the equations

$$\left.\begin{array}{l} P^{'}_{\nu_e\nu_\mu}(\theta^{'}_{13}, \delta^{'}) = P_{\nu_e\nu_\mu}(\theta_{13}, \delta) \\ P^{'}_{\bar\nu_e\bar\nu_\mu}(\theta^{'}_{13}, \delta^{'}) = P_{\bar\nu_e\bar\nu_\mu}(\theta_{13}, \delta) \end{array}\right\} \tag{7}$$

have solutions in the allowed physical range.

It turns out that there are generically two fake sign solutions to eqs. (7). It is very easy to find them in the vacuum approximation, as they mirror the two solutions (true and fake) obtained in the analysis of the intrinsic degeneracies. It can be seen in eq. (1) that a change in the sign of Δm^2_{13} can be traded in vacuum by the substitution $\delta \to \pi - \delta$ [18], implying then for eqs. (7)

$$P^{'}_{\nu_e\nu_\mu(\bar\nu_e\bar\nu_\mu)}(\theta^{'}_{13}, \delta^{'}) \simeq P_{\nu_e\nu_\mu(\bar\nu_e\bar\nu_\mu)}(\theta^{'}_{13}, \pi - \delta') \,, \tag{8}$$

in the vacuum approximation. Consequently, the solutions in vacuum can be obtained from those present for the intrinsic case, upon the substitution $\delta' \to \pi - \delta'$. One of them mirrors

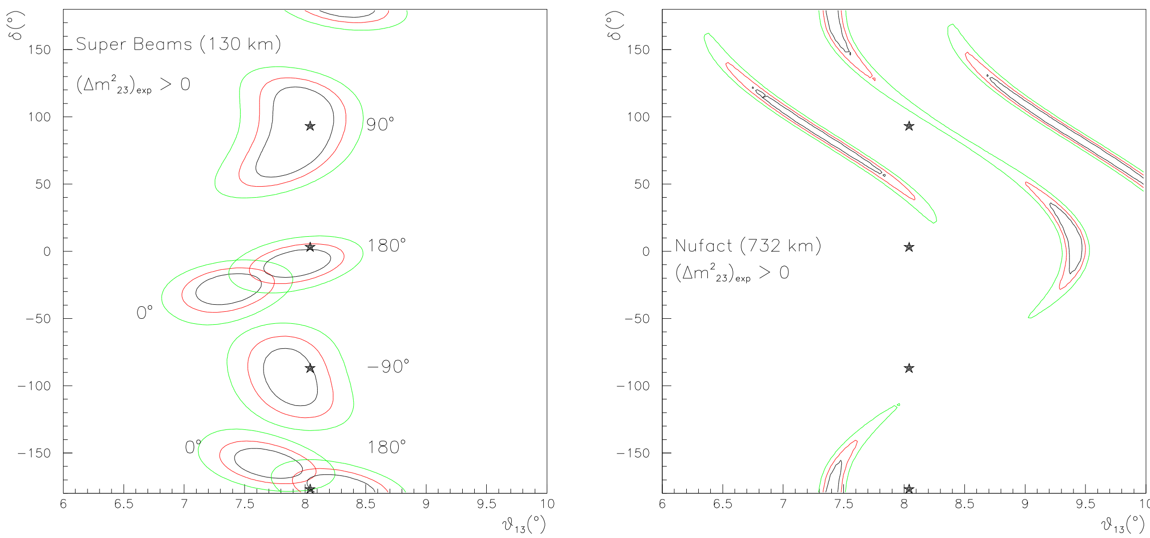

Figure 5: *Fits for central values $\theta_{13} = 8°$ and $\delta = -90°, 0°, 90°, 180°$ for the SPL-SB (left) and NF at $L = 732$ km (right). Nature's sign for Δm^2_{23} is assumed to be positive, while the fits have been performed with the opposite sign. All fake solutions disappear when the two sets of data are combined.*

the true (nature) solution and will be called below solution I, given in vacuum by

$$\begin{aligned} \delta' &\simeq \pi - \delta, \\ \theta'_{13} &\simeq \theta_{13}. \end{aligned} \tag{9}$$

The fact that it is approximately E- and L-independent suggests that it will be hard to eliminate it by exploiting the L, E dependence of different facilities, as indeed is confirmed by the fits below. Fortunately, this fake solution does not interfere significantly with the determination of θ_{13} or CP-violation (i.e. $\sin\delta$).

The second fake sign solution, which we will call solution II, can be read in vacuum from eqs. (5) and (6), upon the mentioned $\delta' \to \pi - \delta'$ exchange. It is strongly L- and E-dependent. Both solutions I and II can be nicely seen in the numerical analysis for the SPL-SB in Fig. 5 (left), for $\theta_{13} = 8°$ and positive sign(Δm^2_{13}).

Matter effects are obviously very important in resolving fake sign solutions[19]: the task should thus be easier at large θ_{13} and large enough NF baselines, where matter effects are largest[10]. In fact it is easy to prove that no solutions can remain for large enough θ_{13}. This can be seen in Figs. 6, which show the fake sign solutions as they result from solving numerically eqs. (7) (using the approximate probabilities with matter effects included [14])

[10] We have checked that for the sign degeneracies (and only for these), the combined results from a SB facility and a NF baseline at $L = 7332$ km are competitive or even superior to those obtained in the combination with an intermediate NF baseline.

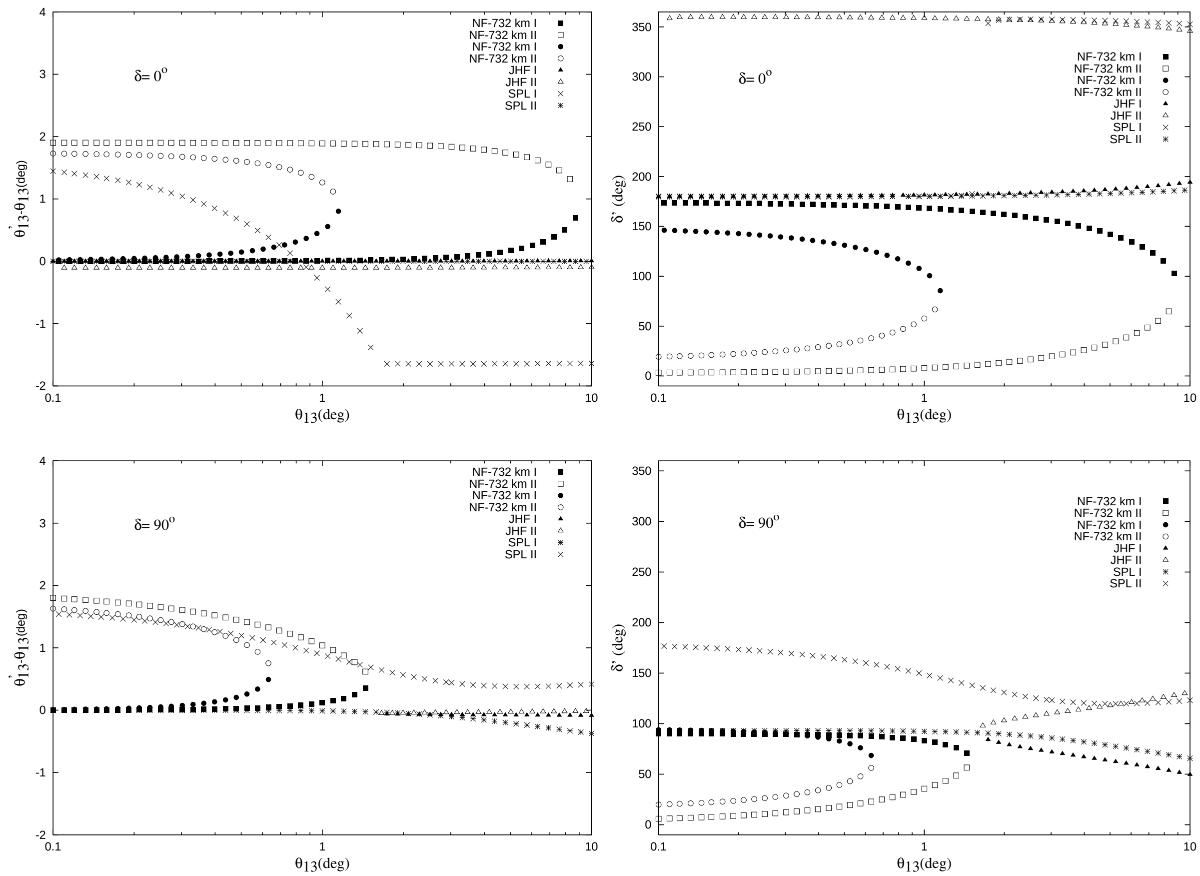

Figure 6: $\theta'_{13} - \theta_{13}$ *(left) and* δ' *(right) for the sign degeneracies as functions of* θ_{13} *for fixed values of* $\delta = 0^\circ$ *(up) and* $\delta = 90^\circ$ *(down). Solutions* I *and* II *are described in the text.*

for the different experiments. For small θ_{13} the two solutions I and II exist in all cases, while for large θ_{13} they degenerate and disappear because of matter effects. One should keep in mind, though, that even if no fake solution exists, there might be approximate ones that will show up in a measurement with finite errors.

Our fits including realistic background errors and efficiencies confirm the above expectations, at each given facility. To be more precise, we have found no fake sign solution for values of $\theta_{13} > 2^\circ$, when considering just one NF baseline of $L = 2810$ km (or longer), while for $2^\circ > \theta_{13} > 1^\circ$ they do appear but get eliminated when the data are combined with those from the SPL-SB. At $L = 732$ km some fake sign solutions remain close to the present experimental limit for θ_{13}, as shown in Figs. 5 (right). It should be noticed that, again, in the combination of these latter data with those from the SPL-SB facility, all fake sign solutions disappear for large $\theta_{13} \geq 4^\circ$, and the sign of Δm^2_{13} could thus be determined from it.

Figures 6 also illustrate that solution I is more facility-independent than solution II, as argued above. The solutions that survive in the combinations for small θ_{13} are indeed of type

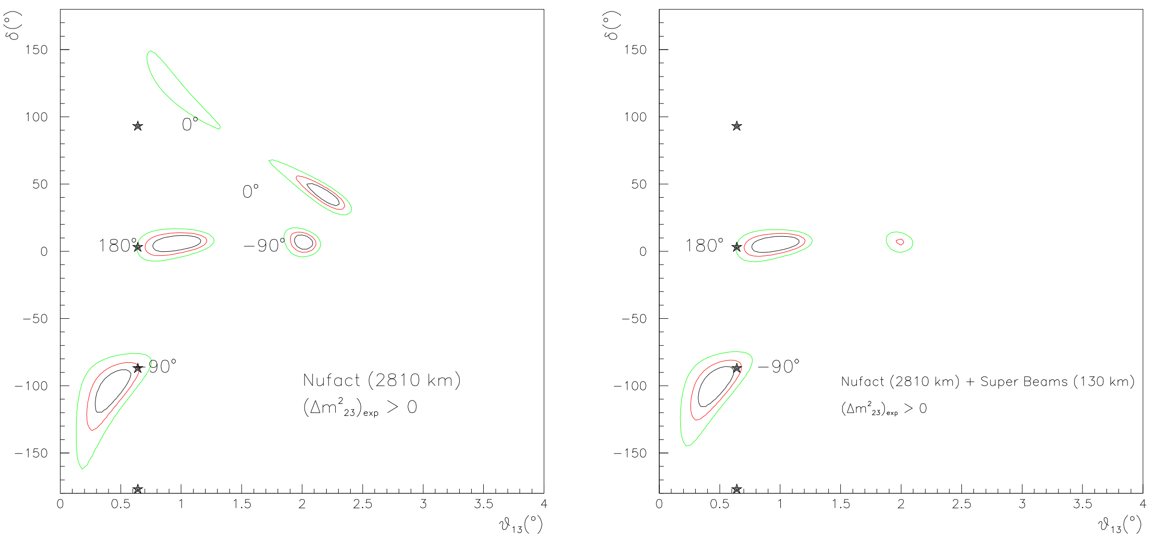

Figure 7: *Fits resulting in fake sign solutions, for central values* $\theta_{13} = 0.6^\circ$ *and* $\delta = -90^\circ, 0^\circ, 90^\circ, or 180^\circ$. *The nature sign for* Δm^2_{13} *is positive, while the fits have been performed with the opposite sign. The results from an NF baseline at* $L = 2810$ *km can be appreciated on the left, while their combination with data from the SPL-SB facility can be seen on the right.*

I, as shown in Figs. 7 [11].

In conclusion, in the LMA-SMW regime, the sign of Δm^2_{13} can be determined from data at an intermediate or long NF baseline alone for θ_{13} well inside the atmospheric regime. For the larger values of θ_{13}, the combination of data from the SB facility and a $L = 732$ km NF baseline also results in no fake sign solutions.

With lowering θ_{13} ($\theta_{13} > 1^\circ$ for our central parameters), the sign can still be determined through the combination of SB and NF data at the intermediate or long distance.

Finally, for the range $\theta_{13} < 1^\circ$, the sign cannot be determined, but the combination of data from the SB facility and an intermediate (or long) NF baseline is still important to reduce the fake solutions to those of type I, which do not interfere significantly with the determination of θ_{13} and δ.

Concerning the dependence on the solar parameters, we do not expect that the conclusions will change very much with lower $\sin 2\theta_{12}\Delta m^2_{12}$. The argument for solutions of type II parallels that given in the previous section for the intrinsic fake solution, while the existence and position of the type I solutions is pretty insensitive to the solar parameters.

[11] In the same exercise, but with the opposite sign of Δm^2_{13}, which leads to larger statistics, solution II disappears completely.

5 $\theta_{23} \to \pi/2 - \theta_{23}$ degeneracy

The present atmospheric data indicate that θ_{23} is close to maximal, although not necessarily $45°$. Superkamiokande results [20] give 90%CL-allowed parameter regions for $\sin^2 2\theta_{23} > 0.88$, translating into the allowed range $35° < \theta_{23} < 55°$. Therefore even if the value of $\sin^2 2\theta_{23}$ is determined with great accuracy in disappearance measurements, there may remain a discrete ambiguity under the interchange $\theta_{23} \leftrightarrow \pi/2 - \theta_{23}$. If this θ_{23} ambiguity is not cleared up by the time of the NF operation, supplementary fake solutions [9] may appear when extracting θ_{13} and δ, when the wrong choice of octant is taken for θ_{23}. Fake solutions follow from solving the system of equations, for fixed L and E_ν:

$$\left.\begin{array}{l} P''_{\nu_e\nu_\mu}(\theta'_{13}, \delta') = P_{\nu_e\nu_\mu}(\theta_{13}, \delta) \\ P''_{\bar\nu_e\bar\nu_\mu}(\theta'_{13}, \delta') = P_{\bar\nu_e\bar\nu_\mu}(\theta_{13}, \delta) \end{array}\right\} \quad , \tag{10}$$

where $P''_{\nu_e\nu_\mu}$ denotes the oscillation probabilities upon the exchange $\theta_{23} \leftrightarrow \pi/2 - \theta_{23}$.

It turns out that, within the allowed range for the parameters, there are generically two solutions to these equations. They should converge towards the true solution and its intrinsic degeneracy, in the limit $\theta_{23} \to \pi/4$. We will thus denote again solution I that which mirrors nature's choice and solution II that which mirrors the intrinsic degeneracy. Because of this parenthood, solution I is *a priori* expected to present generically less L and E dependence than solution II, and be thus more difficult to eliminate in the combination.

It is easy and simple to obtain the analytical form of the fake degeneracies in the vacuum approximation, in which, from eqs. (1) we get

$$\begin{aligned} P''_{\nu_e\nu_\mu(\bar\nu_e\bar\nu_\mu)}(\theta'_{13}, \delta') &= c_{23}^2 \sin^2 2\theta'_{13} \sin^2 \tfrac{\Delta m^2_{13} L}{4E} + s_{23}^2 \sin^2 2\theta_{12} \sin^2 \left(\tfrac{\Delta m^2_{12} L}{4E}\right) \\ &+ \tilde{J}' \cos\left(\delta' \mp \tfrac{\Delta m^2_{13} L}{4E}\right) \tfrac{\Delta m^2_{12} L}{4E} \sin\left(\tfrac{\Delta m^2_{13} L}{4E}\right) . \end{aligned} \tag{11}$$

Let us consider in turn the atmospheric and solar regimes. For large θ_{13}, fake θ_{23} solutions are given by

$$\begin{aligned} \sin\delta' &\simeq \cot\theta_{23} \sin\delta, \\ \theta'_{13} &\simeq \tan\theta_{23}\, \theta_{13} + \frac{\sin 2\theta_{12} \frac{\Delta m^2_{12} L}{4E}}{2\sin\left(\frac{\Delta m^2_{13} L}{4E}\right)} \left(\cos\left(\delta - \tfrac{\Delta m^2_{13} L}{4E}\right) - \tan\theta_{23} \cos\left(\delta' - \tfrac{\Delta m^2_{13} L}{4E}\right)\right) \end{aligned} \tag{12}$$

This system describes two solutions. For one of them (I) the L- and E- dependent terms in eqs. (12) tend to cancel for $\theta_{23} \to \pi/4$, resulting in ${\theta_{13}}' = \theta_{13}$, $\delta' = \delta$ in this limit. The other solution (II) coincides in this limit with that for the intrinsic degeneracy, eq. (5), as expected. For both fake θ_{23} solutions, deep in the atmospheric regime the shift $\theta'_{13} - \theta_{13}$ is positive (negative) for $\theta_{23} > (<) \pi/4$. Note also that, from eqs. (12), no fake solutions are expected for $|\cot\theta_{23} \sin\delta| > 1$. In the plots of Figs. 8 and 10, we show the solutions to eqs. (10), including matter effects, for θ_{23} at the two extremes of the 90%CL-allowed interval. Note that for large θ_{13} there is one solution (I) that is more facility-independent than the other, although the E, L dependence is sizeable for both solutions (see for instance the curves for $\delta = 90°$ in Figs. 10) when θ_{23} is so far from maximal.

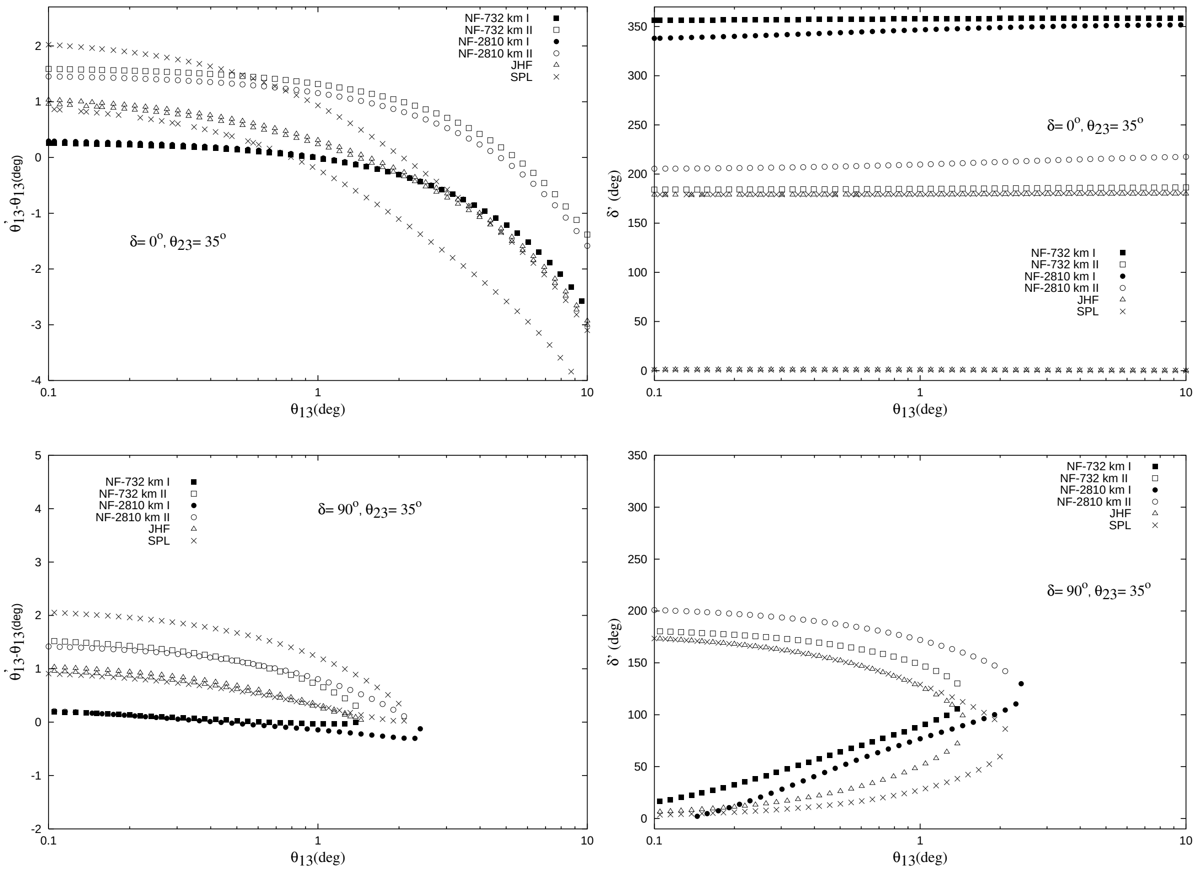

Figure 8: $\theta_{13}^{'} - \theta_{13}$ *(left) and* δ' *(right) for the* θ_{23} *fake solution as functions of* θ_{13}*, for* $\theta_{23} = 35°$*, for fixed values of* $\delta = 0°$*(up) and* $\delta = 90°$ *(down).*

We have performed fits with the wrong choice of octant for θ_{23} and central values of θ_{23} at the limit of the currently allowed domains. The results confirm the expectations above and indicate a situation close to that for the fake sign degeneracies, albeit slightly more difficult. For instance, at the $L = 2810$ km baseline of the NF alone, still some fake θ_{23} solutions remain down to $\theta_{13} > 2°$, but again they all disappear when combined with the SPL-SB data. As an illustration, in Figs. 9 we show the results for $\theta_{23} = 35°$ and $\theta_{13} = 4°$, at the SPL-SB facility (left) and the $L = 2810$ km NF baseline (right). The same exercise, but for an $L = 732$ km baseline of the NF, results in the elimination of the θ_{23} degeneracies only for $\theta_{13} \geq 8°$.

Let us now turn to the study of the solar regime. For $\theta_{13} \to 0°$, there are again two fake solutions if the following condition is met:

$$\tan^2 \theta_{23} < \frac{1}{\sin^2\left(\frac{\Delta m_{13}^2 L}{4E}\right)}. \tag{13}$$

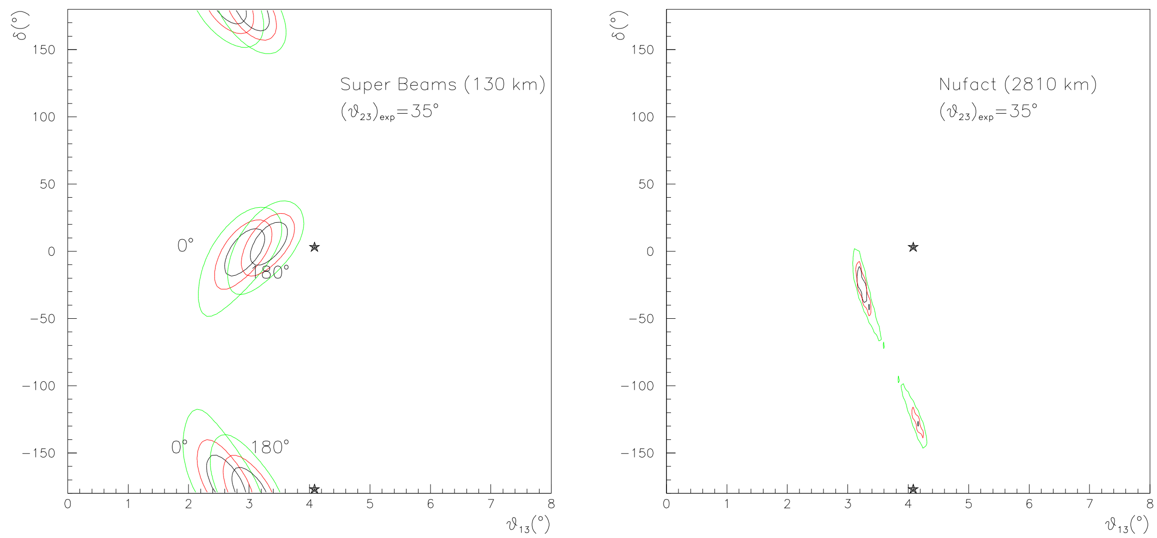

Figure 9: *Fake solutions due to θ_{23} degeneracies for SPL-SB results (left) and a $L = 2810$ km NF baseline (right), for $\theta_{23} = 35°$, $\theta_{13} = 4°$ and $\delta = -90°, 0°, 90°, 180°$. The combination of the results from both experiments resolves the degeneracies.*

Otherwise no solution exists. This is important for the larger possible values of θ_{23} and well reflected in Figs. 10, which show the exact solutions for $\theta_{23} = 55°$. Indeed no fake θ_{23} degeneracies appear in the SB facilities in this case, for θ_{13} in the solar regime.

For $\theta_{13} \to 0°$, eqs. (10) can be easily solved to first order in $\epsilon_{23} \equiv \tan\theta_{23} - 1$. Solution I becomes in this limit:

$$\left.\begin{array}{l} \text{if } \cos 2\theta_{23} \cot\left(\frac{\Delta m^2_{13} L}{4E}\right) > 0 \text{ then } \delta' \simeq 0 \\ \text{if } \cos 2\theta_{23} \cot\left(\frac{\Delta m^2_{13} L}{4E}\right) < 0 \text{ then } \delta' \simeq \pi \end{array}\right\} \quad \theta'_{13} \simeq \sin 2\theta_{12} \frac{\Delta m^2_{12} L}{4E} \left|\epsilon_{23} \csc\left(\frac{\Delta m^2_{13} L}{2E}\right)\right|. \tag{14}$$

Similarly, solution II for $\theta_{13} \to 0°$ is given by:

$$\left.\begin{array}{l} \text{if } \cot\left(\frac{\Delta m^2_{13} L}{4E}\right) > 0 \text{ then } \delta' \simeq \pi \\ \text{if } \cot\left(\frac{\Delta m^2_{13} L}{4E}\right) < 0 \text{ then } \delta' \simeq 0 \end{array}\right\} \quad \theta'_{13} \simeq \sin 2\theta_{12} \frac{\Delta m^2_{12} L}{4E} \left(\left|\cot \frac{\Delta m^2_{13} L}{4E}\right| \pm \epsilon_{23} \cot \frac{\Delta m^2_{13} L}{2E}\right), \tag{15}$$

where the sign $\pm$ corresponds to the sign($\cot \frac{\Delta m^2_{13} L}{4E}$). The intrinsic degeneracy, eq. (6), is recovered for $\theta_{23} = 45°$. Note that, in the solar regime both fake θ_{23} solutions have a sizeable L, E dependence, when θ_{23} is far from maximal. These two solutions can be seen in Figs. 8 and 10 for small θ_{13}. Only for the NF setups do solutions I and II remain on the same curve in the solar and atmospheric regimes. In the case of the SPL and JHF facilities, they are mixed.

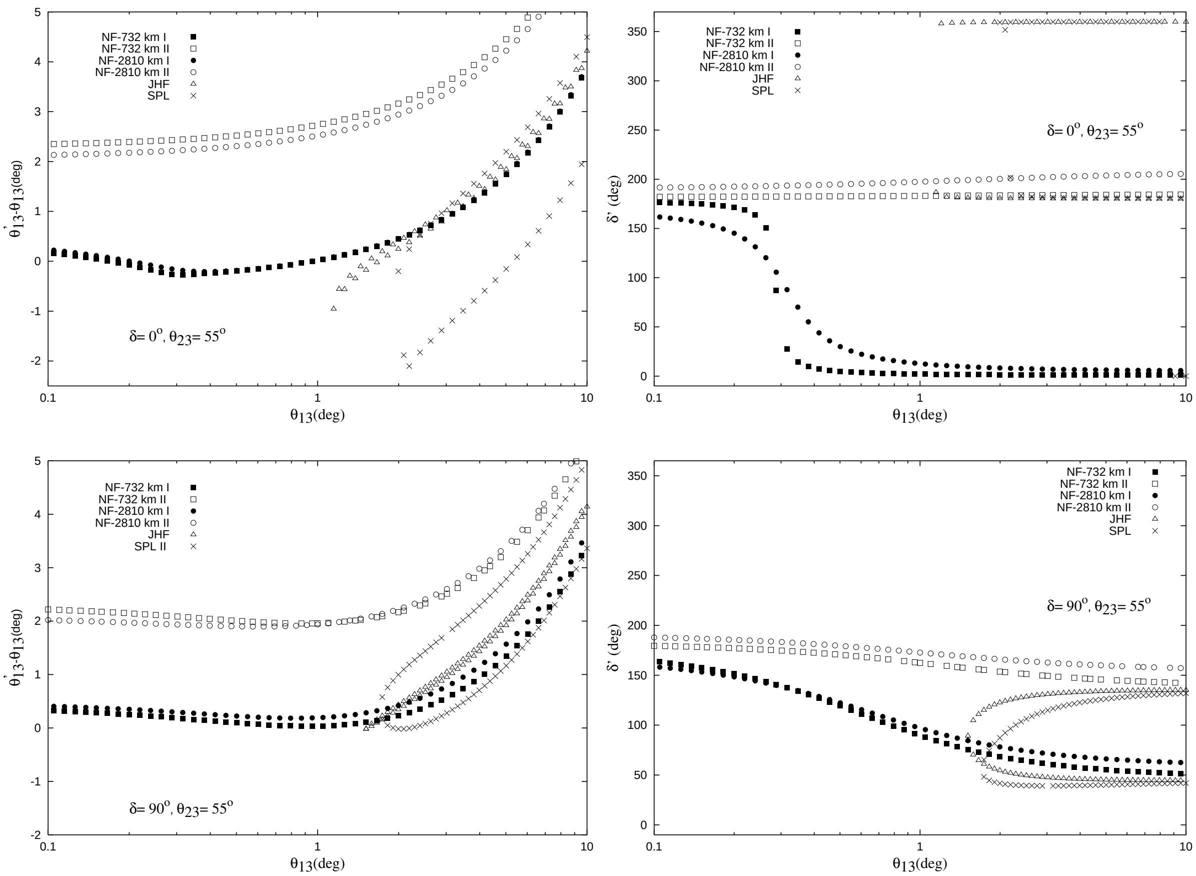

Figure 10: $\theta'_{13} - \theta_{13}$ *(left) and* δ' *(right) for the intrinsic fake solution as a function of* θ_{13}*, for* $\theta_{23} = 55°$*, for fixed values of* $\delta = 0°$ *(up) and* $\delta = 90°$ *(down).*

Figures 11 show the fits for $\theta_{13} = 0.6°$, for a NF at $L = 2810$ km (left) as well as the same combined with the results from the SPL-SB facility (right): only one annoying fake solution remains in the latter, which results from the merging of solution I for SB and solution II for the NF, owing to the finite resolution. See eqs. (14) and (15).

In general we have found that the NF and SPL-SB combination brings an enormous improvement to the solution of these fake degeneracies, particularly for large θ_{13}. The conclusions are rather parallel to those for the fake sign(Δm^2_{13}) solutions, with the caveat that for the θ_{23} ambiguities, solution I, which is harder to resolve, is not that close to satisfying $\sin \delta' = \sin \delta$, and it is thus potentially more harmful to the measurement of CP violation.

As regards the dependence on the solar parameters, the arguments of the previous two sections can be repeated for solutions I and II, when θ_{23} is close to maximal. When θ_{23} is farther from $\pi/4$, the situation is more confusing since both solutions have a dependence on the solar parameters and a detailed exploration of the whole LMA parameter space is necessary.

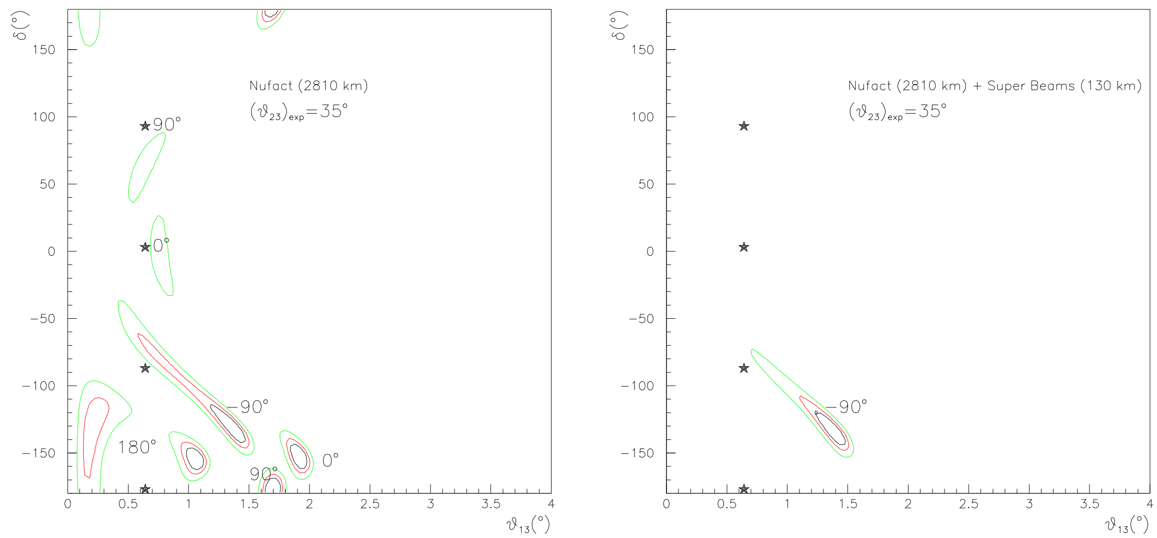

Figure 11: *As Figs. (7) but for the case of θ_{23} degeneracies.*

6 The silver channels

One possibility that can help very much to remove degeneracies further is to measure also the $\nu_e \to \nu_\tau$ and $\bar{\nu}_e \to \bar{\nu}_\tau$ transition probabilities. The relevance of these *silver* channels in reducing intrinsic degeneracies was studied in ref. [11], in the atmospheric regime. Consider the approximate oscillation probabilities[14, 11, 22] in vacuum for $\nu_e \to \nu_\tau$ ($\bar{\nu}_e \to \bar{\nu}_\tau$):

$$\begin{aligned} P_{\nu_e\nu_\tau(\bar{\nu}_e\bar{\nu}_\tau)} &= c_{23}^2 \sin^2 2\theta_{13} \sin^2\left(\frac{\Delta m_{13}^2 L}{4E}\right) + s_{23}^2 \sin^2 2\theta_{12} \left(\frac{\Delta m_{12}^2 L}{4E}\right)^2 \\ &- \tilde{J} \cos\left(\pm\delta - \frac{\Delta m_{13}^2 L}{4E}\right) \frac{\Delta m_{12}^2 L}{4E} \sin \frac{\Delta m_{13}^2 L}{4E}. \end{aligned} \tag{16}$$

They differ from those in eq. (1) by the interchange $\theta_{23} \to \pi/2 - \theta_{23}$ and by a change in the sign of the interference term.

For the intrinsic degeneracies in the atmospheric regime, it follows that the sign of $\theta_{13}^{'} - \theta_{13}$ will be opposite to that for the golden $\nu_e \leftrightarrow \nu_\mu$ ($\bar{\nu}_e \leftrightarrow \bar{\nu}_\mu$) channels given in eqs. (5). In the solar regime, the intrinsic solutions in these silver channels will thus be identical to eqs.(6) upon exchanging $\delta' = 0$ and π, and the combination of the golden and silver channels remains a promising option.

Let us now turn to the fake θ_{23} solutions. When considering only $\nu_e \to \nu_\tau$ and $\bar{\nu}_e \to \bar{\nu}_\tau$ oscillations, the location of the fake solutions related to the θ_{23} ambiguity, in the atmospheric regime, is:

$$\begin{aligned} \sin\delta^{'} &\simeq \tan\theta_{23} \sin\delta, \\ \theta_{13}^{'} &\simeq \cot\theta_{23}\ \theta_{13} - \sin 2\theta_{12} \frac{\frac{\Delta m_{12}^2 L}{4E}}{2\sin\frac{\Delta m_{13}^2 L}{4E}} \left(\cos\left(\delta - \frac{\Delta m_{13}^2 L}{4E}\right) - \cot\theta_{23} \cos\left(\delta^{'} - \frac{\Delta m_{13}^2 L}{4E}\right)\right) \end{aligned} \tag{17}$$

Thus the shift $\theta'_{13} - \theta_{13}$ at large θ_{13} would have the opposite sign to that in eq. (12).

In the solar regime, on the other hand, solution I for the ν_τ appearance measurement is the same as that in eq. (14), while solution II is different, namely:

$$\left.\begin{array}{l} \text{if } \cot\left(\frac{\Delta m^2_{13} L}{4E}\right) > 0 \text{ then } \delta' \simeq 0 \\ \text{if } \cot\left(\frac{\Delta m^2_{13} L}{4E}\right) < 0 \text{ then } \delta' \simeq \pi \end{array}\right\} \quad \theta'_{13} \simeq \sin 2\theta_{12} \frac{\Delta m^2_{12} L}{4E} \left(\left|\cot \frac{\Delta m^2_{13} L}{4E}\right| \mp \epsilon_{23} \cot \frac{\Delta m^2_{13} L}{2E} \right). \tag{18}$$

The condition for the existence of solutions in the solar regime is also different:

$$\cot^2 \theta_{23} < \frac{1}{\sin^2\left(\frac{\Delta m^2_{13} L}{4E}\right)}. \tag{19}$$

A detailed analysis for a realistic experimental setup will be done elsewhere [23], but we expect that the combination of the two appearance measurements: $\nu_e \to \nu_\mu$ and $\nu_e \to \nu_\tau$ for both polarities can help to resolve the dangerous solution I associated with the θ_{23} ambiguity, for θ_{13} in the atmospheric regime.

Finally, we recall that the disappearance measurements (e.g. $\nu_\mu \to \nu_\mu$) should also be helpful in reducing these ambiguities for large θ_{23}. Obviously, if the angle θ_{23} will turn out to be close to maximal (as the best-fit point now indicates), the θ_{23} degeneracies will be of very little relevance.

As for the removal of the fake sign(Δm^2_{13}) degeneracies, the *silver* channels will also help, for qualitatively the same reason as in the combination of facilities with opposite value of $\cot \frac{\Delta m^2_{13} L}{4E}$. For maximal θ_{23}, the solution of type I in the silver channel is the same in vacuum as that in the golden channel, and it is thus not expected to disappear in the combination of the two appearance measurements. The solution of type II, instead, has an opposite displacement in θ_{13} in the atmospheric regime and a difference of 180° in the phase in the solar one.

7 Conclusions

The extraction of a given set of nature values (θ_{13}, δ) from the detection of neutrino oscillations through the golden channels $\nu_e \leftrightarrow \nu_\mu$ ($\bar{\nu}_e \leftrightarrow \bar{\nu}_\mu$) results generically in that the true solution may come out accompanied by fake ones, which might interfere severely with the measurement of CP violation. One of the fake solutions comes from the intrinsic correlation between δ and θ_{13}. The others come from the discrete ambiguities: sign(Δm^2_{13}) and sign$(\cos 2\theta_{23})$.

We have shown the enormous potential of combining the data from a superbeam facility and a neutrino factory, to eliminate these degeneracies. Because of the sizeable matter effects, neutrino factory baselines that are optimal to measure CP violation (as well as shorter ones), imply a considerably smaller ratio $\langle L/E \rangle$ than in the proposed superbeam facilities. It turns out that the location of the fake solutions is very sensitive to this quantity, hence the potential of combining the results from both type of facilities.

We have shown that the fake solutions associated with the sign and θ_{23} ambiguities can be grouped in two sets: those closer to nature's values (solutions of type I) and those related to the intrinsic fake solution (solutions II). Generically solutions I show a milder L/E dependence and are thus more difficult to eliminate through this strategy. We have studied all fake solutions both analytically and through simulations, including realistic background errors and efficiencies for a magnetized iron detector at a neutrino factory, and a water Cerenkov one at the proposed SPL superbeam facility.

The fits have been performed assuming the LMA-MSW solar solution, with $\sin^2 2\theta_{12} . \Delta m^2_{12} = 10^{-4}$ eV^2. For θ_{13} near its present limit, the combination of the SPL-SB data and those from a short NF baseline, i.e. $L = 732$ km, is sufficient to resolve all of them and deliver a clean measurement of θ_{13} and leptonic CP violation. With lowering θ_{13} but still in the atmospheric regime, although the same setup often produces interesting results, it is necessary to consider an intermediate NF baseline, i.e. $L = 2810$ km, together with the superbeam. In particular the sign of Δm^2_{13} can be measured from the combination of their data down to $\theta_{13} > 1°$.

For values of $0.5° < \theta_{13} < 1°$ most degeneracies still disappear in the combined data from the SPL-SB facility and the $L = 2810$ km NF baseline, but some fake solutions remain, mainly of type I. While those associated to the sign$(\frac{\Delta m^2_{13} L}{4E})$ ambiguity bias only slightly the extraction of the true θ_{13} and δ values, those related to θ_{23} would remain a problem, if θ_{23} were far from maximal.

A simultaneous error on the assumed sign(Δm^2_{13}) and θ_{23} octant, of course, gives rise to additional combined fake solutions: we have checked, for our central values of the oscillation parameters, that those get resolved when the corresponding individual degeneracies get resolved. Besides, although we have not done a systematic exploration of the presently allowed range for the atmospheric and solar parameters, we have argued that we expect conclusions similar to those obtained in this work, for lower values of Δm^2_{13} and Δm^2_{12}, to the extent that the sign of $\cot\left(\frac{\Delta m^2_{13} L}{4E}\right)$ remains opposite in the two facilities.

It has previously been pointed out [11] that a supplementary measurement of the *silver* channels, i.e. $\nu_e \leftrightarrow \nu_\tau$ ($\bar{\nu}_e \leftrightarrow \bar{\nu}_\tau$), could help in removing the intrinsic degeneracy. We have also discussed in this paper the expected impact of such measurements on resolving the fake sign and θ_{23} degeneracies. Although a detailed analysis will be done elsewhere, we expect a big improvement in eliminating in particular the dangerous fake solutions associated with the θ_{23} octant ambiguity.

Superbeams and Neutrino Factory are two successive steps in the same path towards the discovery of leptonic CP violation: a golden path, not so much for its budgetary cost, but for the solid and shining perspective offered by the combination of their physics results.

8 Acnowledgements

We are indebted to Andrea Donini and Stefano Rigolin for useful discussions and comments. The work of M.B. Gavela and J.J. Gómez-Cadenas was partially supported by CICYT projects FPA 2000-0980 (GCPA640), and SPA2001-1910-C03-02 , respectively. That of O. Mena and P. Hernández was partially supported by AEN-99/0692.

References

[1] SNO collaboration, arXiv:nucl-ex/0204008 and arXiv:nucl-ex/0204009.

[2] L. Wolfenstein, Phys. Rev. **D 17** (1978) 2369 and **D 20** (1979) 2634. S.P. Mikheyev and A. Yu. Smirnov, Sov. J. Nucl. Phys. **42** (1986) 913.

[3] For a recent analysis, see for instance J. Bachall, M.C. González-García and C. Peña-Garay, arXiv:hep-ph/0204314.

[4] B. Richter, arXiv:hep-ph/0008222. H. Minakata, H. Nunokawa, Phys. Lett. **B495** (2000) 369 [arXiv:hep-ph/0004114]. K. Dick *et al.*, Nucl. Phys. **B598** (2001) 543 [arXiv:hep-ph/0008016]. V. Barger *et al.*, Phys. Rev. **D63** (2001) 113011 [arXiv:hep-ph/0012017].

[5] M. Mezzetto, CERN-NUFACT-NOTE-60.

[6] J. J. Gómez-Cadenas *et al.*, arXiv:hep-ph/0105297.

[7] S. Geer, Phys. Rev. D **D57** (1998) 6989 [Erratum,ibid.˙**D59** (1998) 039903] [arXiv:hep-ph/9712290]. A. De Rújula, M. B. Gavela and P. Hernández, Nucl. Phys. **B547** (1999) 21 [arXiv:hep-ph/9811390]. For a comprehensive set of further references and a recent review, see O. Yasuda, arXiv: hep-ph/0111172 and J.J. Gómez-Cadenas and D. Harris, FERMILAB-PUB-02-044-T, to appear in An. Rev. Mod. Phys.

[8] J. Burguet-Castell *et al.*, Nucl. Phys. **B608** (2001) 301 [arXiv:hep-ph/0103258].

[9] V. Barger, D. Marfatia and K. Whisnant, Phys. Rev. **D65** (2002) 073023.

[10] M. Freund, P. Huber and M. Lindner, Nucl. Phys. **B615** (2001) 331, [arXiv:hep-ph/0105071]; P. Huber, M. Lindner and W. Winter, arXiv:hep-ph/0204352.

[11] A. Donini, D. Meloni and P. Migliozzi, arXiv:hep-ph/0206034.

[12] V. Barger, D. Marfatia and K. Whisnant, arXiv:hep-ph/0206038.

[13] A. Cervera, F. Dydak and J.J. Gómez-Cadenas, Nucl. Instrum. Meth. **A451** (2000) 123.

[14] A. Cervera *et al.*, Nucl. Phys. **B579** (2000) 17; Erratum,ibid. **B593** (2001) 731.

[15] A. Blondel, M. Donega and S. Gilardoni, CERN-NUFACT-NOTE-078.

[16] Y. Itow *et al.*, arXiv:hep-ex/0106019.

[17] P. Zucchelli, arXiv:hep-ex/0107006.

[18] H. Minakata, H. Nunokawa and S. Parke, arXiv: hep-ph/0204171.

[19] V. Barger *et al.*, Phys. Lett. **B485** (2000) 379.

[20] T. Toshito, arXiv:hep-ex/0105023.

[21] R. Gandhi *et al.*, Astropart. Phys. **5** (1996) 81.

[22] M. Freund, Phys. Rev. **D64** (2001) 053003. K. Kimura, A. Takamura and H. Yokomakura, arXiv: hep-ph/0203099 and arXiv: hep-ph/0205295.

[23] A. Donini *et al.*, private comunication.